Title

MEASUREMENT OF DEUTERIUM BEAM ENERGY DISTRIBUTION AND SPECIES USING AN ELECTROSTATIC ENERGY ANALYZER

Authors

Wekhof, A.
Smith, R.R.
Medley, S.S.

Publication Date

1982-05-01

LBL-14435
Preprint

Lawrence Berkeley Laboratory
UNIVERSITY OF CALIFORNIA

Accelerator & Fusion Research Division

Submitted to Nuclear Technology/Fusion

MEASUREMENT OF DEUTERIUM BEAM ENERGY DISTRIBUTION AND SPECIES USING AN ELECTROSTATIC ENERGY ANALYZER

A. Wekhof, R.R. Smith, and S.S. Medley

May 1982

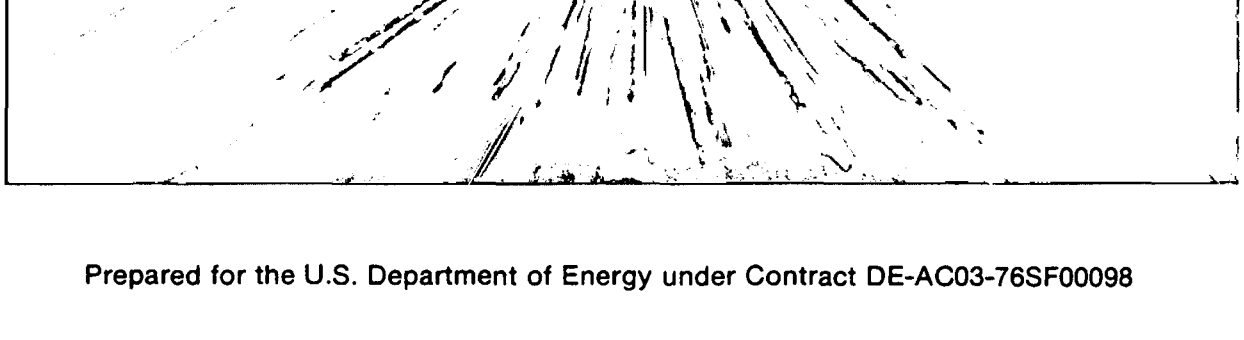

Prepared for the U.S. Department of Energy under Contract DE-AC03-76SF00098

DISCLAIMER

LBL-14435

Measurement of Deuterium Beam Energy Distribution and Species Using an Electrostatic Energy Analyzer*

A. Wekhof and R. R. Smith

Lawrence Berkeley Laboratory
University of California
Berkeley, CA 94720

and

S. S. Medley

Princeton University
Plasma Physics Laboratory
Princeton, New Jersey 08544

---

* This work was supported in part by the Director, Office of Energy Research, Office of Fusion Energy, Development and Technology Division, of the U. S. Department of Energy under Contract No. DE-AC03-76-SF-00098, and in part under (PPPL) Contract No. DE-AC02-76-CH0-3073.

ABSTRACT

The peak energy, energy broadening, and neutral current fractions for the E, E/2, and E/3 energy components of the prototype TFTR 120 keV deuterium neutral beam source were measured on the Neutral Beam System Test Facility (NBSTF) at the Lawrence Berkeley Laboratory (LBL) using a 127° swept electrostatic energy analyzer provided by the Princeton Plasma Physics Laboratory (PPPL). The results were compared with Doppler shift spectroscopy measurements, taking into account the different geometrical factors for both methods. The average neutral current fractions for the E, E/2, and E/3 atomic species components measured with the electrostatic analyzer and extrapolated to the target area were 0.35, 0.47, and 0.18, respectively, which agreed with the spectroscopic results to within 5%. For all species a 1/e full width energy broadening of $\Delta E/E \cong 4\%$ was observed both for an analyzer energy resolution of ~4% and 1%. This width is not in contradiction with the energy broadening expected due to Frank-Condon dissociation effects. The peak energies for the E, E/2, and E/3 components were within ~ 4% of the rated values, but consistently on the low side of the standard deviation.

I. INTRODUCTION

The ion sources used for powerful neutral beam heating in fusion experiments typically produce both atomic and molecular ions of D^+, D_2^+, and D_3^+ which subsequently convert to deuterium atoms having energies at full (E), one half (E/2), and one third (E/3) the value of the initial acceleration energy. In both the development and application of neutral beam injectors, the peak energy, energy width, and neutral current associated with the E, E/2, and E/3 components are essential parameters for determining the performance of the neutral beam injector. The purpose of the present experiment was to make direct measurements of the deuterium neutral beam components using an Electrostatic Analyzer (ESA) and to compare the results with Doppler shift spectroscopy data obtained with the use of an Optical Multichannel Analyzer (OMA). For several years, the OMA diagnostic [1] has been used on the Neutral Beam System Test Facility (NBSTF) [2] to provide convenient computerized data acquisition and analysis. Independent ESA measurements provide a useful corroboration of the OMA data since the two methods are subject to different geometrical and calibration factors which affect interpretation of the measured neutral beam parameters.

II. THE ELECTROSTATIC ANALYZER (ESA)

Since the construction and calibration of the electrostatic analyzer have been documented elsewhere [3], only a summary of the important features is presented in this section. Also discussed are: 1) installation and alignment of the ESA on the NBSTF, and 2) modifications to the ESA which were made as a result of operating experience.

The 127° electrostatic analyzer is shown schematically in Fig. 1 along with the aperture in the NBSTF target tank calorimeter through which the analyzer views the ion source. Component dimensions relevant to the analyzer performance characteristics are given in Table I.

For cylindrical plates with an outer radius of r_2 (applied potential +V) and inner radius r_1 (applied potential -V), a singly charged ion of energy

$$E = eV/\ln (r_2/r_1) , \tag{1}$$

follows a circular path through entrance and exit apertures located on the plate centerline $r_o = (r_2 - r_1)/2$. Using a 0-150 keV H^+ ion beam with energy calibration accurate to ± 1% and 0-10 kV deflection plate power supply voltages calibrated to ± 0.1%, the experimental relation between plate voltage and transmitted energy was measured as:

$$E = 18.74\ V - 0.18 \tag{2}$$

where V, E are in units of kV and keV, respectively.

The energy as a fraction of the centroid value resolution is approximated by treating the plate entrance and exit apertures as slits of width W_1 and W_2, respectively. The transmitted beam intensity will take the form of a trapezoid with a base width of $(W_1 + W_2)/r_o$ and a top width of $(W_2 - W_1)/r_o$ giving a full width at half maximum of

$$\frac{\Delta E}{E} = \frac{W_2}{r_o} . \tag{3}$$

TABLE I

COMPONENT DIMENSIONS

FOR THE LBL 127° ELECTROSTATIC ANALYZER

COMPONENT	DIMENSIONS
ENTRANCE DEFLECTION PLATES	
LENGTH	5.0 cm
SEPARATION	1.0 cm
STRIPPING CELL	
LENGTH	12.5 cm
ENTRANCE DIAMETER	0.1 cm
EXIT DIAMETER	0.2 cm
CYLINDRICAL ANALYZER PLATES	
OUTER RADIUS (R_2)	20.5 cm
INNER RADIUS (R_1)	19.5 cm
EXIT APERTURE A.	0.8 cm
B.	0.2 cm

During calibration an exit aperture of 0.08 cm was used which for r_0 = 20 cm gives an energy resolution of 0.4% in good agreement with the measured energy resolution [3]. For reasons to be discussed later, during operation on the NBSTF the analyzer exit aperture was increased to 0.8 cm giving an energy resolution of $\Delta E/E$ = 4% for the species measurements presented in this report. For the final measurements of species energy distributions this exit aperture was decreased to 0.2 cm.

The stripping cell efficiency was inferred from measurements using an ion beam (~ 10 μA at 120, 60, and 40 keV) with the aid of a combination Faraday cup and secondary emission detector. Using a stripping cell length, ℓ = 12.5 cm, and nitrogen stripping gas at a gauge reading pressure of p = 5 mTorr, the measured stripping efficiency was found to agree well with the analytic expression [4,5]:

$$\eta_{01} = F_{1\infty} \exp[-\ell C_1 G p \sigma_s] \times \{1 - \exp[-\ell C_1 G p(\sigma_{01} + \sigma_{10})]\} \quad (4)$$

where C_1 = 3.243×10^{13} cm^{-3} mTorr^{-1},

P = cell pressure (mTorr),

ℓ = cell length (cm),

G = pressure correction due to the ionization gauge factor corresponding to the cell gas,

σ_{01} = stripping cross section (cm^2),

σ_{10} = electron capture cross section (cm^2),

σ_s = scattering cross section (cm^2),

$F_{1\infty}$ = equilibrium fraction.

In this expression, the equilibrium fraction [6]

$$F_{1\infty} = \frac{\sigma_{01}}{\sigma_{01} + \sigma_{10}} \tag{5}$$

is used because the values can be measured with an uncertainty of ±5% whereas the individual cross section are known to within only ± 20%.

For nitrogen gas G = 1 was adopted and cross sections σ_{01} and σ_{10} were obtained from the ORNL compilation of cross section data [6].

Due to the lack of published data on the total scattering cross section, σ_s, for hydrogenic particles on nitrogen gas a derived empirical expression was used [3]:

$$\sigma_s = 1.9 \times 10^{16} \times 10^{\alpha(E)} cm^2, \tag{6}$$

where

$$\alpha(E) = - 0.64113 \log (1.602 \times 10^{-9} E) - 4.80524 \tag{7}$$

and E is the incident hydrogen energy in keV.

III. THE OPTICAL MULTICHANNEL ANALYZER (OMA)

The technique of Doppler shift spectroscopy for powerful neutral beam diagnostics using an Optical Multichannel Analyzer (OMA) was reported earlier [1]. In this section we describe the procedure by which the OMA results are used to deduce the current ratios of the neutral beam species expected at the entrance of the ESA for comparison with like measurements made using the ESA method.

The comparison of the beam species ratios measured by the OMA and the ESA techniques is somewhat indirect and model dependent. The former method is spatially integrated over most of the beam in a plane roughly 0.75 meters from the source, while the latter method looks through a sequence of apertures 12 meters from the source. The ESA not only samples a small fraction of the beam entering the target tank, but also views only a small portion of the source. Because the various ionic and neutral species have different divergences, presumably due to the dissociation energy of di- and triatomic ions, the prediction of the neutral currents entering the ESA involves both a geometric correction and also a correction for the evolution of the species through the neutralizer.

Comparison of the two measuring techniques is made with the aid of Fig. 2. At a position 0.75 m from the source a collection of mirrors brings light emitted in a plane perpendicular to the accelerator's extraction slots as well as light emitted in a plane parallel to the slots simultaneously to a Spex monochromator. The two viewing angles are chosen such that the perpendicular light is shifted to longer wavelengths. The perpendicular view samples the entire 40 cm height of the source in a band roughly 5 cm wide, and the parallel view samples the entire 10 cm width of the source in a band through the midplane roughly 5 cm high. The Doppler shifted light emitted by

atoms of full, one half, and one third the accelerating potential are simultaneously viewed in the parallel and perpendicular directions for a total of six peaks relevant to the species measurement. For small deviations of an atom's path from the beam axis, the spectral distribution of the emitted light is a measure of the angular distribution of the atoms. We observe that each peak is well described by a Gaussian distribution raised to a fractional power, although the physical cause for this is not clear at present. Thus for three atomic species, two planes of view, and both a 1/e width and an exponent for each peak, there are a total of twelve geometric parameters measured by the OMA.

The relative proportions of the integrals under each peak are interpreted as the relative proportions of D^+, D_2^+, and D_3^+, extracted from the accelerator by using a particular model for the creation of excited states which emit D_α light [7]. This model is rather insensitive to the assumed neutralizer thickness. Then the analytic solutions given by the ORNL neutral beam group [8], for the evolution of the eleven positive and neutral species are used to compute the total currents of atoms exiting the neutralizer.

The four geometric parameters for each specie are then used to make a geometric correction. Because the range of divergences accepted by the detector is so narrow, it is not necessary to integrate in spherical coordinates the angular distribution emitted from each source point toward the limiting aperture of the detector. Instead, it is sufficient to use the zero angle value of the angular distribution function. This value is inversely proportional to the product of the integrals of the independent parallel and perpendicular distributions. Because of the narrowness of these distributions, the integrations from $-\pi/2$ to $+\pi/2$ can be replaced with integrations from $-\infty$ to $+\infty$, leading to three pairs of normalization factors of the form $K = d/[w\Gamma(1/2d)]$, where Γ is the gamma function.

Finally, the predicted neutral currents are combined with the geometric corrections and renormalized to give the proportions of full, one half, and one third energy atoms entering the electrostatic analyzer.

IV. THE EXPERIMENTAL ARRANGEMENT ON THE NBSTF

The ESA was installed on the rear side of the NBSTF Target Tank as shown schematically in Fig. 2. The ESA views the ion source grids at a distance of 12.9 meters from the entrance of the stripping cell through an aperture in the target tank calorimeter at 2.0 meters.

The axis of the ESA, defined by the entrance and exit apertures of the stripping cell, was aligned with the neutral beam axis by using a telescope to locate the "center" of the ion source grids while viewing through a 3/8 inch diameter aperture in the target tank calorimeter. The area of the source viewed by the limiting apertures of the stripping cell was a circle of 5 cm diameter.

In order to minimize the thermal loads on the analyzer components, the aperture in the test tank calorimeter was set at 3/8" diameter. During initial tests, however, it was discovered that thermally induced distortion of the calorimeter displaced the aperture producing a shuttering effect observed by reduction of the ESA signal. This was corrected by enlarging the calorimeter aperture to a diameter of 1.0 inches.

A potential of 5 kV was applied across the deflection plates preceeding the stripping cell for the two-fold purpose of removing ions formed due to reionization of the neutrals along the beamline and quenching excited states of the atomic neutrals.

To obtain time resolved energy measurements during a neutral beam pulse, the cylindrical plate potentials were swept using an HP-85 computer to program voltage waveforms fed to a KEPCO D/A converter (0 - 10 V) which in turn drives a pair of TREK Model 606 high voltage operational amplifiers (0 - 10 kV) to provide the ± V voltages required to scan the E, E/2, and E/3 beam energy components. This voltage programming enabled the plate voltage to be stepped and relatively slowly scanned over each beam energy component to avoid distortion of the signals resulting from circuit RC time constants. The high voltage amplifier and voltage programming systems were checked to determine that no voltage off-sets existed and, using high voltage dividers, the control and amplified voltages were found to track to within 1%.

The original detectors for the analyzed ion beam and the straight-through neutral component were modified from the devices provided by PPPL. During initial operation on the NBSTF, it was observed that the high energy resolution ($\Delta E/E = 0.4\%$) afforded by the 0.08 cm entrance aperture of the Faraday cup ion detector at the exit of the cylindrical analyzer plates apparently produced a deep modulation of the detected signal. This modulation persisted for the case of $\Delta E/E \cong 4\%$ when we used a 0.8 cm aperture as shown in Fig. 3 and Fig. 5. Such a signal is presented in Fig. 3 with an increased time resolution of 10 ms/cm to permit identification of the modulation frequencies.

To detect the neutrals transmitted through an aperture in the outer cylindrical plate we used a secondary emission detector placed inside a copper wire cage. The cathode (secondary emission surface) was heated by means of a tungsten foil during experimental runs in order to minimize any influence of gas and oil films on the secondary electron emission.

The straight through neutral signal from the secondary emission detector and the Faraday cup ion signals were both voltage amplified (RC $\sim$ 10 μsec) near the ESA and cabled from the Target Area to the Control Room for display on either Textronix or Norland 3001 oscilloscopes.

A final point to be discussed before presenting the experimental results concerns stripping cell effects uncovered as a result of operational experience. Only neutrals could enter the gas stripping cell since ions were removed by an entrance deflection plate biased at 5 kV as discussed earlier.

The neutral stripping efficiency is a function of both neutral energy and the stripping cell pressure. If this pressure is large enough, significant scattering of incident neutrals occurs [3] which must be accounted for in the data analysis. The efficiency, η_{01}, for conversion of neutrals into ions was calculated for deuterium atoms incident on nitrogen gas in the pressure range from 0.1 to 1000 mTorr for the full energy specie of 120 keV as well as for the one-half and one third energy components using Eq. (4). As the results plotted in Fig. 4 show, a range of pressure does not exist where all three species have relatively constant stripping efficiency. The absence of an equilibrium is attributed to scattering on the stripping cell gas. The influence of this scattering can be decreased by opening the stripping cell exit aperture or using helium gas which has lower scattering cross sections than N_2 gas. Initially we planned to use helium gas, but later we had to use N_2 gas which is pumped effectively by the beamline cryocondensation pumps. Increasing the cell aperture diameters is restricted, on the other hand, by the need to keep the gas pressure in the analyzer chamber sufficiently low to avoid Paschen breakdown between the high voltage cylindrical plates. As a compromise, the cell entrance and exit apertures were modified to 0.1 and 0.2 cm diameter, respectively. The nitrogen stripping cell was operated

typically at a gauge pressure reading of 40-50 mTorr which gave an actual stripping cell pressure of 5-6 mTorr according to Fig. 4. In fact, the gauge reading and stripping cell pressures were different because of the effect described below.

Using different pressures between 1 and 500 mTorr, the signal amplitude for each of the E, E/2, and E/3 species was measured and plotted as a function of pressure as shown in Fig. 4 by the curves labelled $1^*(E)$, $2^*(E/2)$, and $3^*(E/3)$. One can see that both groups of curves in Fig. 4 are similar in shape, but the experimentally measured curves are shifted toward the region of higher pressure by a factor of 6 to 8. By way of explanation, we note that the ion gauge measures the pressure upstream of the cell at the gas inlet. The true cell pressure is expected to be lower than the gauge reading because of the pressure drop in the interconnecting "tube" between the ion gauge region and the stripping cell. It is difficult to estimate the pressure drop because of two complicating factors. First, the ~ 10 cm long by ~ 1 cm diameter connecting tube is a section of bellows which acts like a series of diaphragms rather than a smooth-walled pipe. Second, the pressure region is intermediate between laminar and molecular flow so that the conductance, L, and hence the pressure drop, $\Delta p = Q \cdot L$, where Q is the gas throughput, is dependent on pressure as given by the Knudsen formula [9]:

$$L = 180 \frac{d^4}{\ell} \bar{p} + 12.1 \frac{d^3}{\ell} \cdot \frac{1 + 256\ d \cdot \bar{p}}{1 + 316\ d \cdot \bar{p}}, \qquad (8)$$

where d(cm), ℓ(cm) are the diameter and length, respectively, the conductance L is in liters/sec and $\bar{p} = 0.5(p_1 + p_2)$ Torr.

where p_1 is the pressure at the tube entrance (in flow direction) and p_2 is the pressure at the tube end. As an example, we take d = 1.0 cm, ℓ = 10.0 cm, $\bar{p} = 10^{-2}$ Torr, and Q = 10 mTorr · ℓ/sec which yields a conductance of L ≅ 1.2 ℓ/sec and a pressure drop of $\Delta p \cong 12$ mTorr. Thus, the pressure drop can be significant but a precise reconciliation of the difference between the calculated and measured results given in Fig. 4 cannot be made.

In fact, molecular free passes λ without collision at the mentioned pressure range (or corresponding densities 10^{13}–10^{15} cm^{-3}) are much more than diagram diameters d, but can be about the tube length ℓ (we assumed neutral collision cross section $\sigma \sim 10^{-16}$ cm^{-2}, [9]). Hence, application of Knudsen formula is still valid, although almost at the limit.

However, the uncertainty introduced into the species ratio measurements us expected to be relatively small since the result depends on the ratios of the stripping efficiencies at E, E/2, and E/3 which depend only slightly on the cell gas pressure as can be seen from Fig. 4. To verify this point, species ratio measurments were made at ion gauge pressure readings of 5 and 40 mTorr to examine the sensitivity of the species ratio measurement to cell pressure.

V. EXPERIMENTAL RESULTS AND DISCUSSION

The ESA measurements were obtained by using computer programmed cylindrical plate voltage waveforms to sweep through the E, E/2, and E/3 beam components as shown in oscillogram A of Fig. 5. An alternative operating mode was to program a constant voltage during the beam pulse in order to observe the temporal behavior of a selected species as shown in oscillograms B, C, and D for the E, E/2, and E/3 species, respectively. In each of the oscillograms A–D, the traces correspond to the swept plate voltage (top), Faraday cup ion

signal (middle), and secondary emission neutral signal (bottom). The ~ 50 msec notch near the end of the signal traces is due to a beam interrupt fault. In oscillograms B-D, the structure on the signal is due to modulation of the beam resulting from 60 Hz and 720 Hz ripple in the ion source power supply. These modulation frequencies are readily identified in Fig. 3 which displays the signal with increased time resolution. The analyzer signal modulation may be due to modulation of the beam divergence which is a sensitive function of the extracted current density and of the electrode voltages. Also noted is a gradual rise in the Faraday cup ion signal (middle traces) and a decrease in the secondary emission neutral signal (bottom traces) which appears less pronounced for the neutral signal because this is a small fractional change in the total neutral signal. This variation is attributed to a change in the effective line density of the stripping cell due to: 1) gas desorption from aperture structures (primarily the stripping cell entrance) produced by impact of energetic beam particles, and 2) accumulation of scattered beam neutrals within the stripping cell. This effect was minimized by collimating the beam at the entrance of the ESA down to a diameter of 0.2 cm, and by decreasing the wall thickness of the leading stripping cell aperture to 0.1 cm. However, residual effects were unavoidable due to the high beam intensity ($\lesssim$ 100 mA/cm^2). The impact on the neutral species ratio measurements were minimized by taking data near the beginning of the beam pulse before appreciable gas build up occurs.

In the middle trace of Fig. 5A, the Faraday cup ion signal shows the energy resolved profile of the E, E/2, and E/3 species, reading from left-to-right. The fourth profile is a repeat of the full energy component. The cylindrical plate voltages were measured corresponding to the peak and 1/e full width of each profile to give the data presented in Table II. The energy

calibration relation given by Eq. (2) then provided the associated energy values. The measured peak energies are within 3.5% of the rated accelerating potentials but are systematically low. The magnitude exceeds the expected accuracy of the accelerating voltage measurements ($\sim$ 1%) and suggests the existence of an energy loss mechanism possibly due to plasma effects in the neutralizer.

The 1/e energy width values given in Table II are not corrected for the ESA instrumental energy resolution which for W_2 = 0.8 cm and r_o = 20 cm is given by Eq. (3) as $\Delta E/E$ = 4%. In the approximation of Gaussian profiles, the observed energy width can be corrected for the instrumental resolution using

$$\Delta_t = (\Delta_m^2 - \Delta_i^2)^{1/2}, \tag{9}$$

where Δ_m is the measured width, Δ_i = 0.04 E_i is the instrumental energy width (E_i = E, E/2, or E/3) and Δ_t is the true beam energy broadening. This procedure yields a Δ_t of 3.91, 1.80 and 1.13 keV for the E, E/2, and E/3 components, respectively.

Due to the Frank-Condon effect, dissociation of the extracted ion molecular species results in a broadening of the ion energy, E, in the laboratory reference frame given by [10]:

$$\Delta E = \pm 2 \sqrt{2E \cdot I} \tag{10}$$

where the potential energy I = 8.3 eV for typical conditions and E, ΔE are in eV. For the 60 and 40 keV beam energy components subject to this effect, the corresponding energy widths from Eq. (10) are $\pm$2.0 and $\pm$1.6 keV which are comparable to the energy resolution of the analyzer. Since similar energy

profile shapes were obtained later with an energy resolution of 1% (0.2 cm analyzer exit aperture)*, these shapes are apparently due to real broadening processes in the beam.

The species ratio measurements were usually taken at constant electrostatic plate voltages in order to minimize errors due to gas pressure build up in the stripping cell and to uncertainty with peak shapes. Constant voltages equal to the measured maximum peak voltage were selected and the signal amplitude was determined by averaging over the first 50-70 msec of the beam pulse when the initial signal oscillations decayed and the ramping of the signal attributed to beam induced increase in the effective stripping cell pressure was not significant. Data were taken with nitrogen ion gauge cell pressure readings of 5 and 40 mTorr, repeating each shot 5 to 7 times. The deviations between shot-to-shot amplitudes for a given series of shots were below 10%. As pointed out earlier, superimposed on the signal for each specie are 60 Hz and 720 Hz oscillations with a modulation level ranging up to 30%. The area under each specie profile was determined graphically and the result convoluted with the appropriate stripping cell efficiency (Fig. 4) to obtain the neutral current ratios at the ESA entrance. The results are presented in Table III along with the OMA data obtained by procedures described earlier.

For this example the relative Faraday Cup currents for the full, half, and one-third energy components, corrected for variations in the neutral signals, are 4.97, 5.16, and 1.65, respectively. The measured stripping cell gauge pressure was 40 mTorr. The stripping cell efficiencies were (Fig. 4) 0.42, 0.29, and 0.22. This gives the incident normalized currents to be 4.97, 7.48, and 3.14, respectively. Renormalizing, this is 32%, 48%, and 20% for the full, half, and one-third energy neutral currents in the target area.

---

* M. C. Vella, private communication.

We measured the distribution of the light in the direction parallel to the grids to be 0.606, 0.307, and 0.087 for the full, half, and one-third energy components. Assuming a neutralizer thickness of 1×10^{16} cm^{-2}, these data imply an extracted current distribution of 0.399, 0.472, and 0.129. The neutral current conversion factors are then computer using the method described above to be 0.411, 1.39, and 2.41 for unit currents of 120 keV D^+, D_2^+, and D_3^+. The full, half, and one-third energy 1/e angles and α parameters are for the parallel direction 0.27°, 0.65; 0.43°, 0.70; and 0.66°, 0.63 and for the perpendicular direction are 0.95°, 0.71; 0.89°, 0.67; 0.95°, 0.52. These imply relative geometric corrections of 1.16, 0.78, and 0.44. Combining the calculated extracted ion distribution, neutral conversion factors, and geometric corrections gives the renormalized neutral current distribution predicted on the basis of the OMA at the entrance to the ESA to be 0.35, 0.50, and 0.14 for the full, half, and one-third energy components.

Reasonable agreement is therefore observed between the results obtained using these two independent methods. Their comparison with other neutral beam species experiments [10, 11] can be difficult because of differences in beamlines and, hence, is not a subject of discussion in this paper.

TABLE II

MEASURED ENERGY PEAK AND WIDTH

FOR 120 KEV DEUTERIUM BEAM COMPONENTS

	120 KEV	60 KEV	40 KEV
PEAK:			
POTENTIAL (VOLTS)	6200 ± 30	3100 ± 15	2070 ± 10
ENERGY (KEV)	116.0 ± 0.6	57.9 ± 0.3	38.6 ± 0.2
WIDTH (1/E):			
POTENTIAL (VOLTS)	340	170	114
ENERGY (KEV)	6.2	3.0	2.0
ENERGY (KEV) CORRECTED FOR ESA ENERGY RESOLUTION	2.8 (0.8)	2.0 (0.5)	1.6 (0.4)

TABLE III

NEUTRAL CURRENTS FOR A 120 KEV DEUTERIUM BEAM

	120 KEV	60 KEV	40 KEV
		ESA RESULTS	
STRIPPING *			
CELL PRESSURE = 5 MTORR	.39	.47	.14
= 40 MTORR	.32	.48	.20
		OMA RESULTS	
NEUTRALIZER			
THICKNESS = 1×10^{16} CM^{-2}	.36	.50	.14
= 6×10^{15} CM^{-2}	.40	.47	.13

* THESE ARE THE GAUGE READINGS, THE REAL STRIPPING CELL PRESSURE IS 6 TO 8 TIMES LESS, SEE FIG. 4.

ACKNOWLEDGMENTS

The work of C. Arthur with the computer software is appreciated by A. Wekhof as well as useful discussions with Mike Vella. The assistance of A. L. Roquemore and J. Thomas during fabrication and calibration of the ESA is gratefully acknowledged by S. S. Medley. All authors appreciate stimulating discussions with Dr. Klaus H. Berkner during the course of the experiment. This work was supported in part by the Director, Office of Energy Research, Office of Fusion Energy, Development and Technology Division, of the U. S. Department of Energy Contract No. DE-AC03-76-SF-00098, and in part under (PPPL) Contract No. DE-AC02-76-CH0-3073.

REFERENCES

[1] C.F. Burrell, W.S. Cooper, R.R. Smith, and W.F. Steele, "Doppler Shift Spectroscopy of Powerful Neutral Beams," Rev. Sci. Instrum., Vol. 51, No. 11, 1451 (1980).

[2] W.B. Kunkel, "Multimegawatt Neutral Beams for Tokamaks," IEEE Trans. on Nucl. Sci., Vol. NS-26, No. 3, 4166 (1979).

[3] S.S. Medley, A.L. Roquemore, and J.-P. Bussac, "High Energy Resolution Electrostatic Energy Analyzer for LBL Neutral Beam Diagnostics," Princeton Plasma Physics Laboratory Report, TFTR-TM-10 (1980).

[4] J.H. Adlam and D.A. Aldcroft, "The Measurement of the Efficiency of a Helium Gas Cell for the Conversion of a Beam of Energetic Atomic Hydrogen into a Proton Beam," Culham Laboratory Report, CLM-R100 (1969).

[5] H. Tawara and A. Russek, "Charge Changing Processes in Hydrogen Beams," Rev. Mod. Phys. 45, No. 2, Part 1, 178 (1973).

[6] C.F. Barnett, et al., Atomic Data for Controlled Fusion Research, ORNL-5206 (Vol. 1), 1977.

[7] J. Hill, J. Geddes, and H.B. Gilbody, J. Phys. B. Atom. Molec. Phys. 13, 951 (1980).

[8] J. Kim and H. H. Haselton, "Analysis of Particle Species Evolution in Neutral-Beam Injection Lines," J. Appl. Phys. 50 (6), 3802 (1979).

[9] Methods of Experimental Physics, Vol. 14 Vacuum Physics and Technology, G.L. Weissler and R.W. Carlson (Ed.), Academic Press (1979) p.15

[10] C.F. Barnett and J.A. Ray, "Beam Specie Analyzer for Intense Neutral Beams," Oak Ridge National Laboratory Report, ORNL/TM-7656 (1981).

[11] S.J. Fielding and D. Stork, "Species and Impurity Measurements in Intense Neutral Beams on the DITE Tokamak," Culham Laboratory Report, CLM-P647 (1981).

FIGURE CAPTIONS

Fig. 1 Schematic of the Electrostatic Analyzer and the target dump area:

1. Deuterium neutral beam.
2. Target dump with a 1 inch diameter aperture.
3. Target vacuum vessel wall and connection with the Electrostatic Analyzer.
4. Electrostatic Analyzer vacuum chamber.
5. Deflection plates with + 5 kV potential.
6. Stripping cell 12 cm long and 1 cm diameter, fed N_2 gas through the bell.
7. Ion gauge for the control of the stripping cell pressure.
8. The Electrostatic Analyzer 127° electrodes.
9. The detector for neutral (non-stripped) component of the beam.
10. Turbomolecular vacuum pump system.
11. Faraday Cup for detection of ion species current.
12. Ion gauge for the control of the base pressure in the analyzer vacuum chamber.

Fig. 2 Flow path diagram depicting the analysis procedure for the Optical Multichannel Analyzer (OMA) and the Electrostatic Analyzer (ESA). The processes captioned in the boxes are described in more detail below using parameter values representative of the experimental measurements.

1. The Doppler shift D_α light emitted by full, half, and one third energy atoms is viewed both parallel and perpendicular to the

accelerator slots. For each of six peaks we measure both a 1/e point and an exponent for an angular distribution function $F(\theta) = K\exp - (\theta/\omega)^{2\alpha}$. For example, we measure the light amplitudes to be .26, .51, .23, the perpendicular ω and α values to be .95°, .71; .89°, .67; .95°, .52; and the parallel divergence parameters to be .27°, .65; .43°, .7; and .66°, .63; for the full, half; and one third energies.

2. Using a model for the creation of excited atoms, the proportions of D^+, D_2^+, and D_3^+ in the emitted beam are computer. With a total neutralizer gas thickness of 1×10^{16} cm^{-2}, we infer .61, .31, .08.

3. Compute the total currents of atoms which exit the neutralizer for a given thickness and initial species mix. For 1 amp of each specie, the currents would be .41, 1.35, and 2.25.

4. Correct for divergence. For each specie and each plane of view, the correction factor $K - \alpha/[\omega \cdot \Gamma (1/2\ \alpha)]$. For this example, the factors are 1.16, .78, and .44 $\times 10^{-8}$ of the total emission. Renormalize the fluxes.

5. Measure the full, half, and one third energy ions through the ESA.

6. Use the stripping coefficient to compute the neutral currents entering the analyzer. Scattering and controlling the N_2 pressure gave difficulty.

7. Compare the measured and computed neutral fluxes. The ESA gave .32-.39, .48-.47, and .20-.14, depending on the stripping cell pressure. The computed values were .36-.40, .50-.47, and .14-.13, depending on the assumed neutralizer thickness.

Fig. 3 Oscillogram illustrating the analyzer swept voltage waveform and the signal modulation observed with high time resolution (10 ms/cm) for $\Delta E/E = 4\%$.

Fig. 4 Calculated and Measured Efficiency Plots.

a. Left scale: Calculated stripping cell efficiency, η_{01}, including scattering for deuterium at 120 keV full energy (curve 1), 60 keV half energy (curve 2), and 40 keV third energy as a function of N_2 stripping gas pressure.

b. Right scale: V^* corresponding to the measured species signal amplitude, V, for the full (curve 1^*), one-half (curve 2^*), and one-third (curve 3^*) energy components as a function of ion gauge pressure readings, in arbitrary units.

Fig. 5 Typical oscillograms of high-voltage ramps applied to the Electrostatic Analyzer plates, Faraday Cup, and Neutral Detector signals for 120 keV Deuterium Neutral Beam (stripping cell N_2 gas pressure P = 10 mTorr).

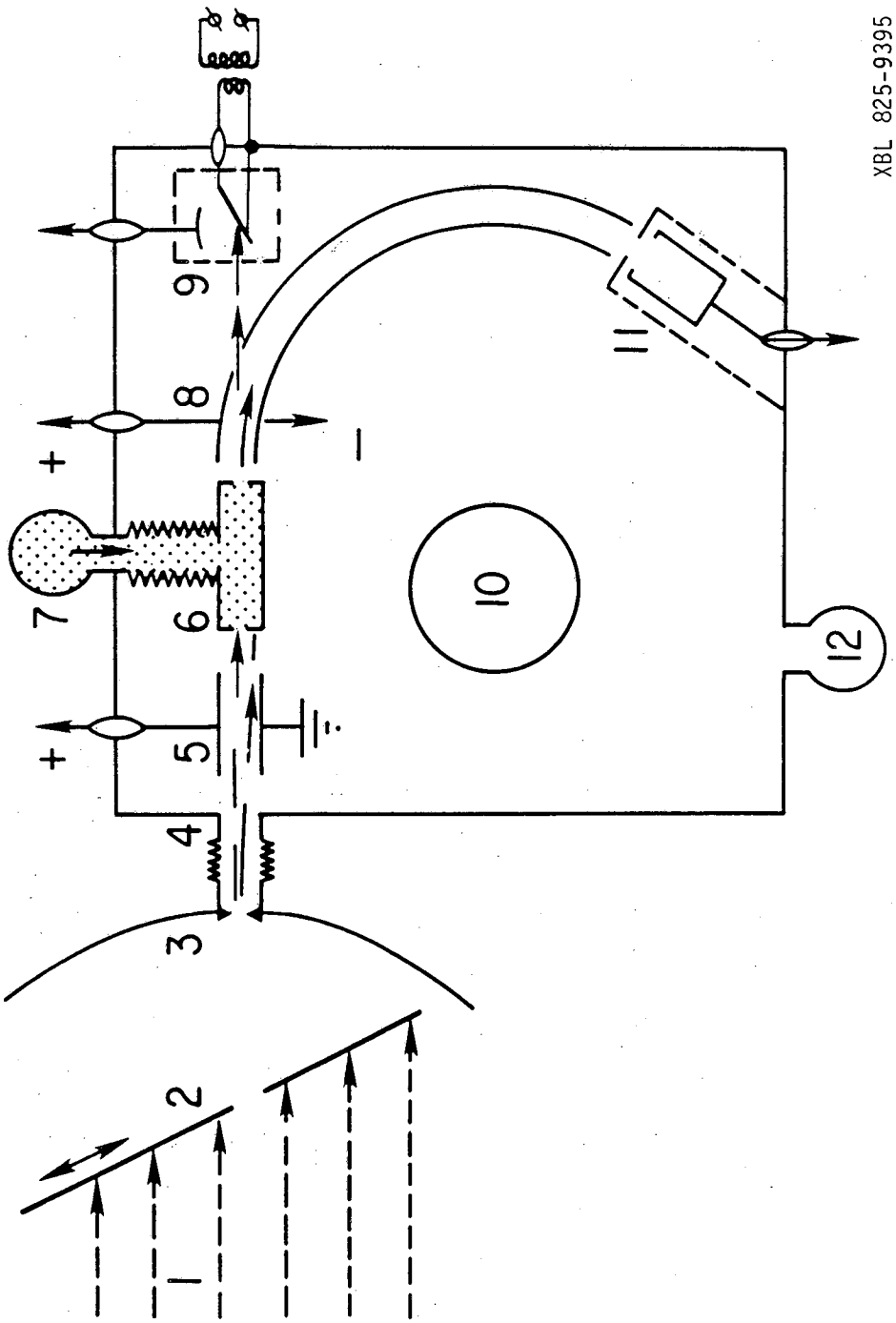

FIGURE 1

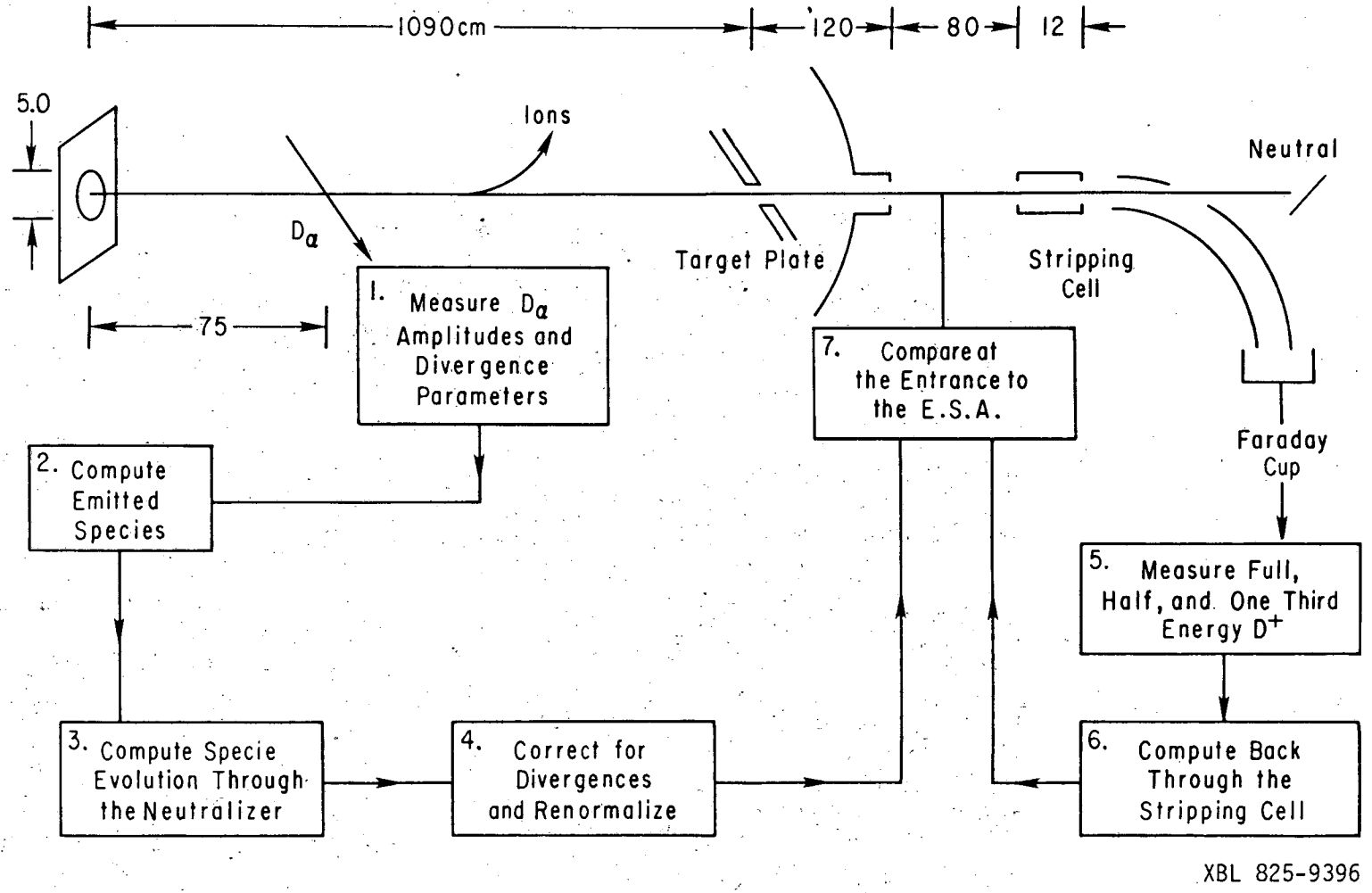
1090cm
120
80
12
5.0
Ions
Neutral
D_α
Target Plate
Stripping Cell
75
1. Measure D_α Amplitudes and Divergence Parameters
7. Compare at the Entrance to the E.S.A.
Faraday Cup
2. Compute Emitted Species
5. Measure Full, Half, and One Third Energy D^+
3. Compute Specie Evolution Through the Neutralizer
4. Correct for Divergences and Renormalize
6. Compute Back Through the Stripping Cell
XBL 825-9396

FIGURE 2

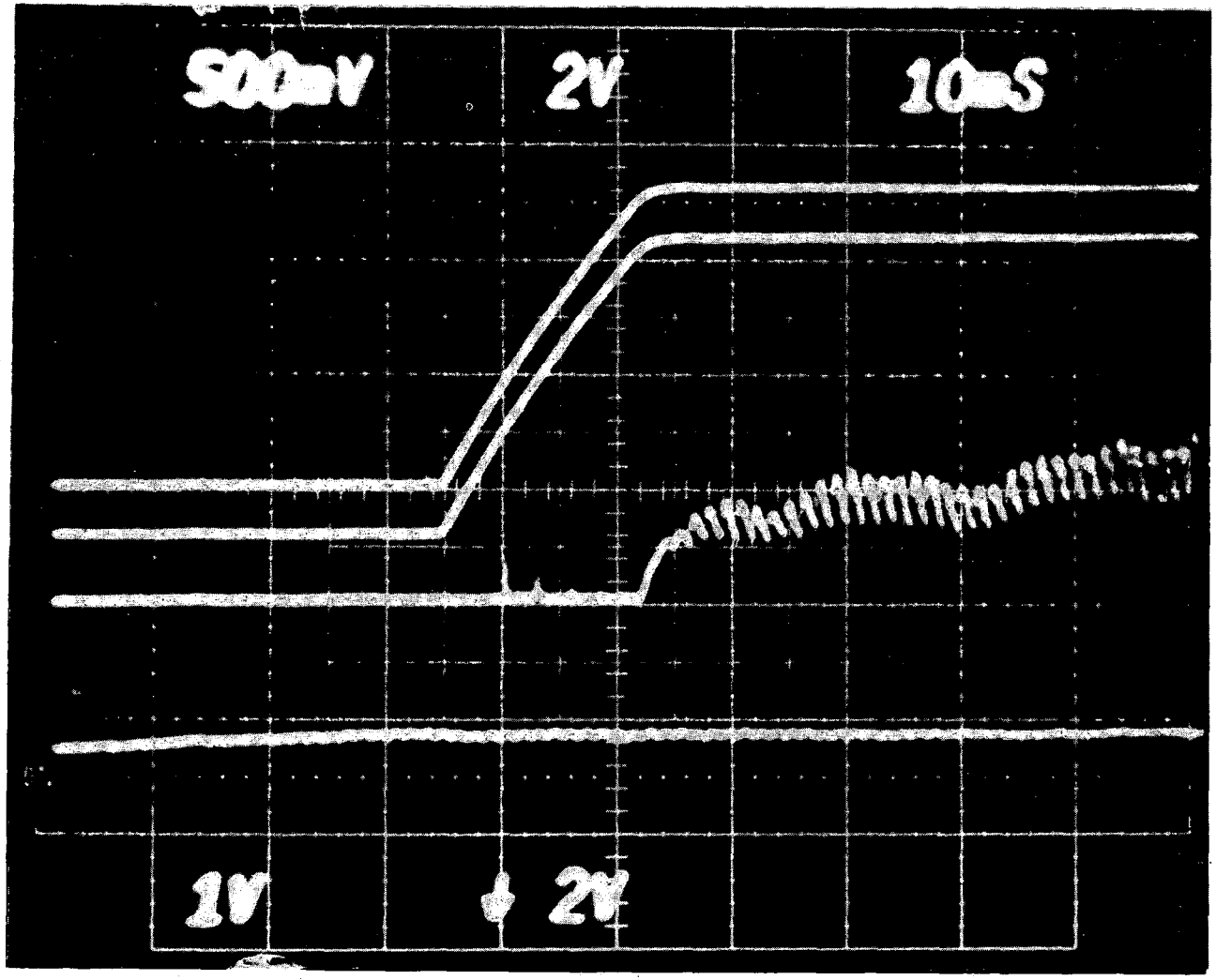

XBB 824 4070

Plate Voltage

Ion Signal

Neutral Signal

FIGURE 3

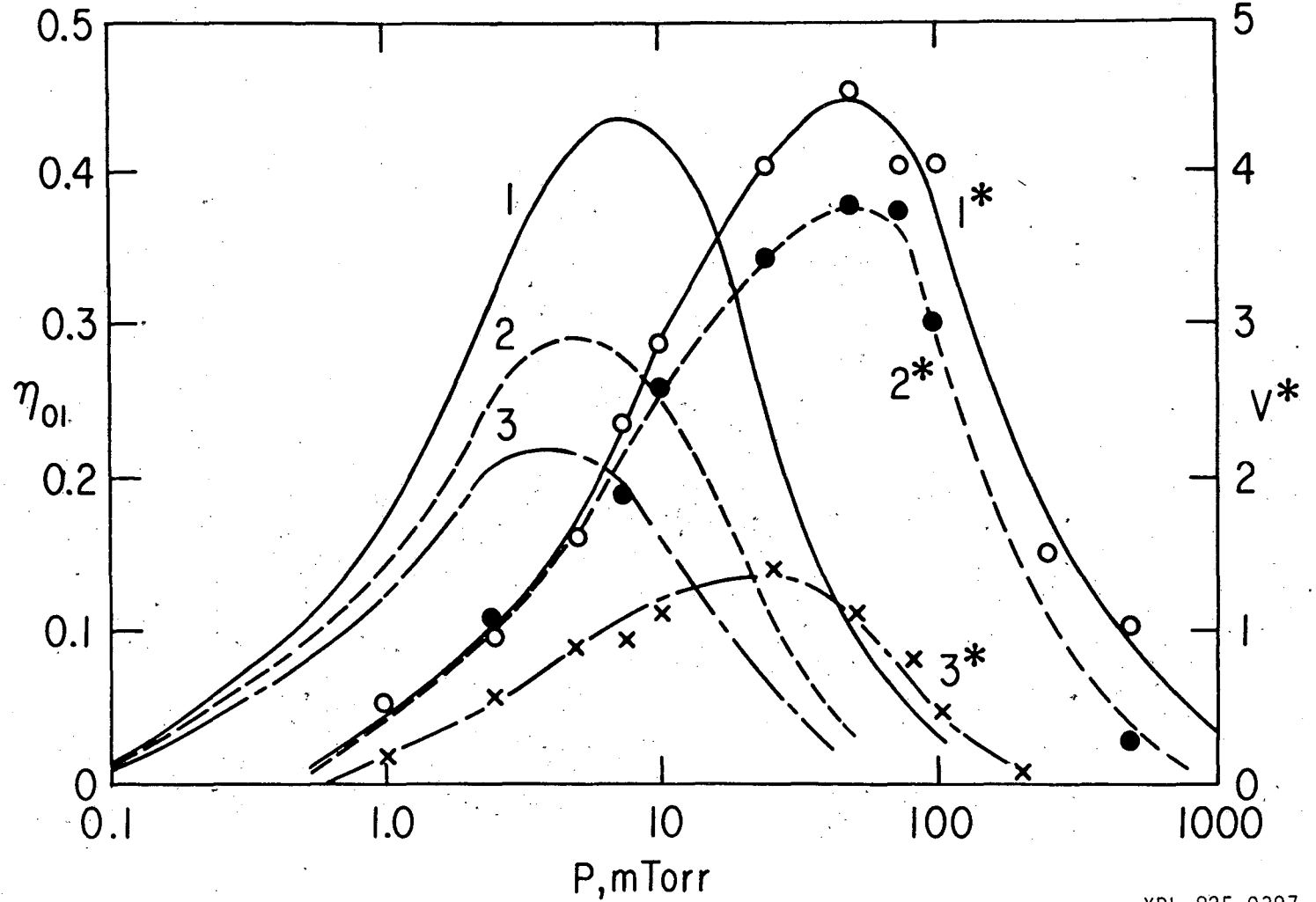

XBL 825-9397

FIGURE 4

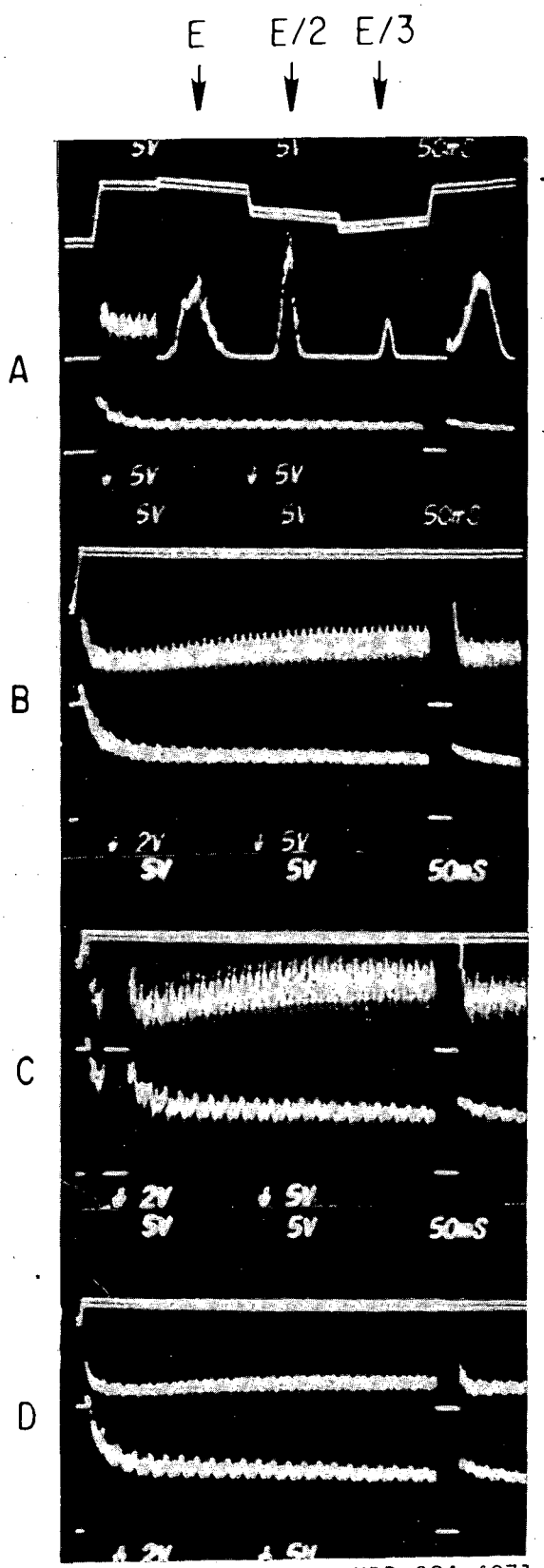

XBB 824-4071

FIGURE 5

TECHNICAL INFORMATION DEPARTMENT
LAWRENCE BERKELEY LABORATORY
UNIVERSITY OF CALIFORNIA
BERKELEY, CALIFORNIA 94720